A deamination-driven biocatalytic cascade for the synthesis of ribose-1-phosphate

Jonas Motter[1], Sarah Westarp[1,2], Jonas Barsig[1], Christina Betz[1], Amin Dagane[1], Felix Kaspar[1,4], Lena Neumair[1], Sebastian Kemper[3], Peter Neubauer[1], and Anke Kurreck[1,2*]

[1]Chair of Bioprocess Engineering, Institute of Biotechnology, Faculty III Process Sciences, Technische Universität Berlin, Straße des 17. Juni 135, D-10623, Berlin, Germany
[2]BioNukleo GmbH, Ackerstraße 76, 13355 Berlin, Germany
[3]Institute for Chemistry, Technische Universität Berlin, Straße des 17. Juni 135, 10623 Berlin, Germany
[4]Institute for Biochemistry, Biotechnology and Bioinformatics, Technische Universität Braunschweig, Spielmannstraße 7, 38106, Braunschweig, Germany
*****Correspondence: anke.wagner@tu-berlin.de

Abstract

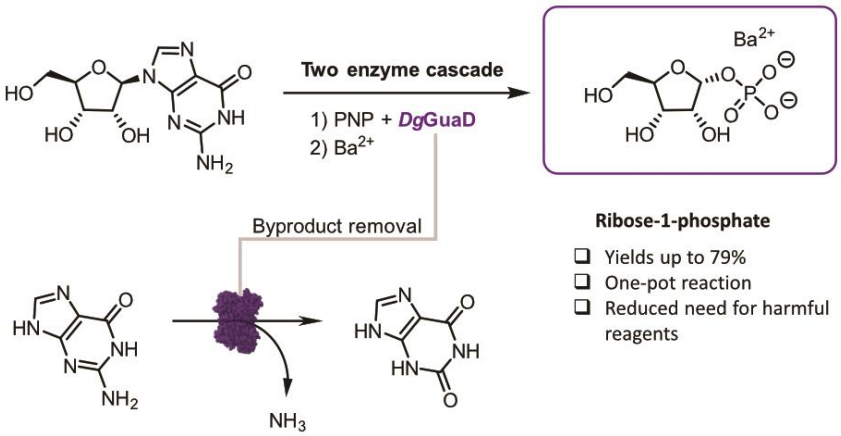

Ribose-1-phosphate (Rib1P) is a key substrate for the synthesis of difficult-to-access nucleoside analogues by nucleoside phosphorylases. However, its use in preparative synthesis is hampered by low yields and low selectivity during its preparation by conventional methods. Although biocatalysis permits straightforward access to Rib1P directly from natural nucleosides, these transformations are tightly thermodynamically controlled and suffer from low yields and non-trivial work-up procedures. To address these challenges, we developed a biocatalytic cascade that allows near-total conversions of natural guanosine into α-anomerically pure Rib1P. The key to this route is a guanine deaminase, which removes the accumulated guanine byproduct. Under optimised conditions, this cascade proved readily scalable to the gram scale, delivering isolated yields of up to 79% and a purity of 94% without any chromatography. Our cascade approach reduced the need for toxic reagents and purification steps inherent to previous methods, reducing the environmental burden of the route, as confirmed by CHEM21 Zero Pass and E-factor calculations. Thus, our work will broadly strengthen the applicability of nucleoside phosphorylase-mediated chemistry.

Introduction

Pentose-1-phosphates (P1Ps), such as ribose-1-phosphate (**Rib1P**), are central molecules in the nucleoside salvage pathway. As substrates for nucleoside phosphorylases (NPs), they additionally serve as valuable starting points for the enzymatic synthesis of nucleoside analogues,[1–7] one of the most successful classes of small-molecule drugs to treat viral infections[8,9] or cancer,[10,11] and which recently attracted interest as precursors of mRNA vaccines[12,13] and antibacterial agents.[14,15] Employing P1Ps for the synthesis of nucleoside analogues is especially advantageous when product

yields are low due to thermodynamic constraints[16–19] or when suitable donor nucleosides are not readily available.[20,21]

Despite its potential for the synthesis of important nucleoside analogues, a high-yielding and sustainable synthesis for P1Ps has not yet been developed. Chemical synthesis routes toward **Rib1P** strongly rely on protection/deprotection steps and show only moderate stereoselectivity, which leads to a mixture of α- and β-anomers.[22] Consequently, only low yields are achieved due to the multi-step synthesis routes and the need for additional purification steps.

Enzymatic and chemoenzymatic approaches using NPs have been developed as a viable alternative, allowing direct biocatalytic access to α-anomeric pure **Rib1P**. NPs catalyse the tightly thermodynamically controlled reversible phosphorolytic cleavage of nucleosides to the corresponding nucleobases and P1Ps.[16–18] Previous NP-based routes toward **Rib1P** are mainly based on natural nucleosides[23–27] or the base-modified 7-methylguanosine (**7-Me-Guo**).[28,29] Using uridine as a substrate for **Rib1P** synthesis, isolated yields of only 31% and 25% were obtained using either *E. coli* UP[23] or thermostable pyrimidine NPs[24] (*Figure 1, Top)***.** The application of **7-Me-Guo** as a substrate offers the advantage of near-irreversible phosphorolysis due to the *in situ* precipitation of the nucleobase and its low nucleophilicity.[28,29]

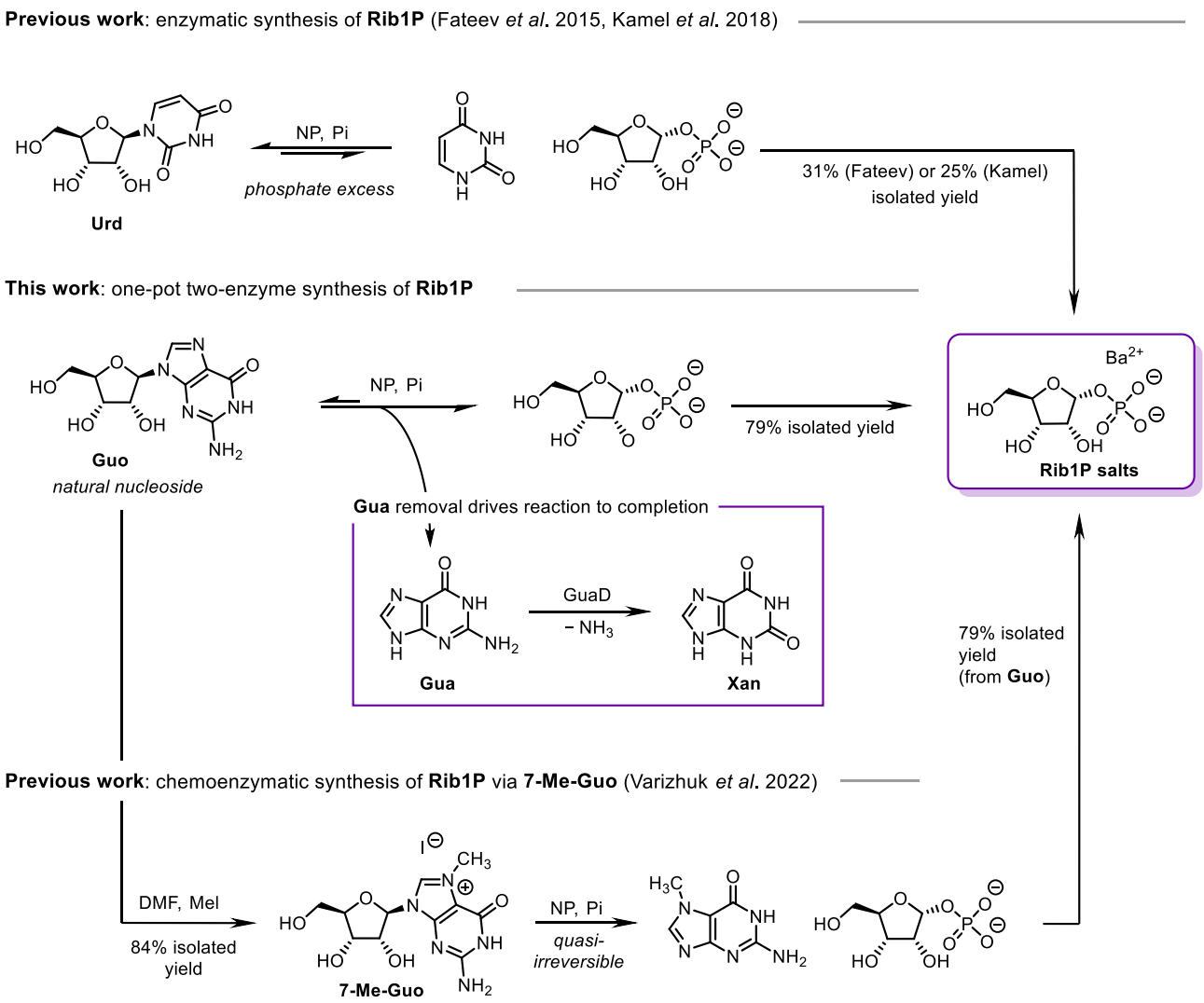

Figure 1. Strategies for the (chemo)enzymatic synthesis of ribose-1-phosphate (**Rib1P**). Top) Enzymatic synthesis by Fateev *et al*. 2015 (ref[23]) and Kamel *et al.* 2018 (ref[24]). Middle) GuaD coupled synthesis as presented in this work. Bottom) Chemoenzymatic synthesis by Varizhuk *et al.* 2022 (ref[29]). **Urd** = uridine, **Guo** = guanosine, **Gua** = guanine.

Whilst total isolated yields of up to 79% (from guanosine, **Guo**) were achieved using the approach, it has the drawback that an upstream chemical step (using toxic and carcinogenic iodomethane) is required to prepare **7-Me-Guo** (*Figure 1, Bottom*). In addition, **7-Me-Guo** is labile to hydrolysis and has a low shelf life, making it a non-ideal reagent.

An *in vitro* biocatalytic cascade involving phosphorolysis and product removal could address these challenges and lead to a high-yielding and sustainable synthesis route of **Rib1P**. Kalckar had already envisioned such a strategy in 1947, by coupling the phosphorolysis of inosine with a xanthine oxidase.[25] Although this approach found a recent application,[27] xanthine oxidases are unstable enzymes and are difficult to produce on scale.[30–35] As such, this vision has not yet been successfully translated into a practical, scalable, high-yielding method that starts from cheap and available substrates and enzymes.

Motivated by these initial efforts, we have developed an enzymatic cascade for the synthesis of **Rib1P** centred around a guanine deaminase (GuaD). Using **Guo** as a substrate for NP-catalysed phosphorolysis permits almost full nucleoside cleavage in the presence of *Deinococcus geothermalis* GuaD (*Dg*GuaD), which converts the accumulating guanine (**Gua**) to xanthine (**Xan**, *Figure 1, Middle*)**.** We herein describe how the application of the thermostable *Dg*GuaD in combination with thermostable NPs allowed the development of a scalable synthesis of **Rib1P** from **Guo** in one pot with isolated yields of up to 79%. These processes benefitted from streamlined purification procedures and led to a strongly reduced need for solvents or hazardous chemicals, which was well reflected by improved values of CHEM21 Zero Pass calculations compared to other (chemo)enzymatic approaches. Thus, our work paves the way for a sustainable synthesis of **Rib1P** and its derivatives, further strengthening the feasibility of biocatalytic nucleoside chemistry.

Results and Discussion

Development of a two-enzyme cascade for Rib1P synthesis

The ideal biocatalytic cascade for **Rib1P** synthesis uses cheap and commercially available starting materials, achieves full conversion of an otherwise thermodynamically controlled reaction, requires only a short reaction time and can be integrated smoothly into downstream processing for product isolation. For these reasons, we envisioned that a cascade starting from **Guo** would offer the best combination of these traits when a deaminase converts the liberated nucleobase **Gua** to poorly soluble **Xan**.

Thus, we began our studies searching for a **Gua**-specific, thermostable guanine deaminase (GuaD, EC 3.5.4.3). Thermostability is considered one of the most critical traits for biocatalysts,[36–40] but previously described narrow-spectrum GuaDs lacked significant stability.[41–43] To this end, we screened genomes of well-described thermophilic organisms for guanine deaminases. We selected GuaD of *D. geothermalis* (*Dg*GuaD) as a promising candidate and heterologously expressed the protein in *E. coli*. A preliminary characterisation of the enzyme revealed that *Dg*GuaD showed a narrow substrate spectrum (only **Gua** is accepted), a high specific enzyme activity (1400 U mg^{-1}), and a moderate thermostability (detailed information on enzyme mining and characterisation is provided in *Figures S1-9*, *Table S1*).

With the specific and thermostable GuaD in hand, we screened reaction conditions for optimal **Rib1P** synthesis. Since **Guo** is a natural substrate for purine NPs (PNPs, EC 2.4.2.1), we decided to use commercially available PNPs from thermophilic microorganisms. Indeed, in coupled reactions of N04 and *Dg*GuaD in the presence of 0.9 equivalents (eq.) of phosphate, we observed up to 80% **Guo** cleavage. Under the same conditions but without GuaD, only 16% conversion is expected based on thermodynamic calculations (K = 0.04 for **Guo** at 50 °C).[16] Hence, byproduct removal led to a significant increase in **Guo** conversion. **Gua** was immediately converted to **Xan** in our cascade reactions and never accumulated.

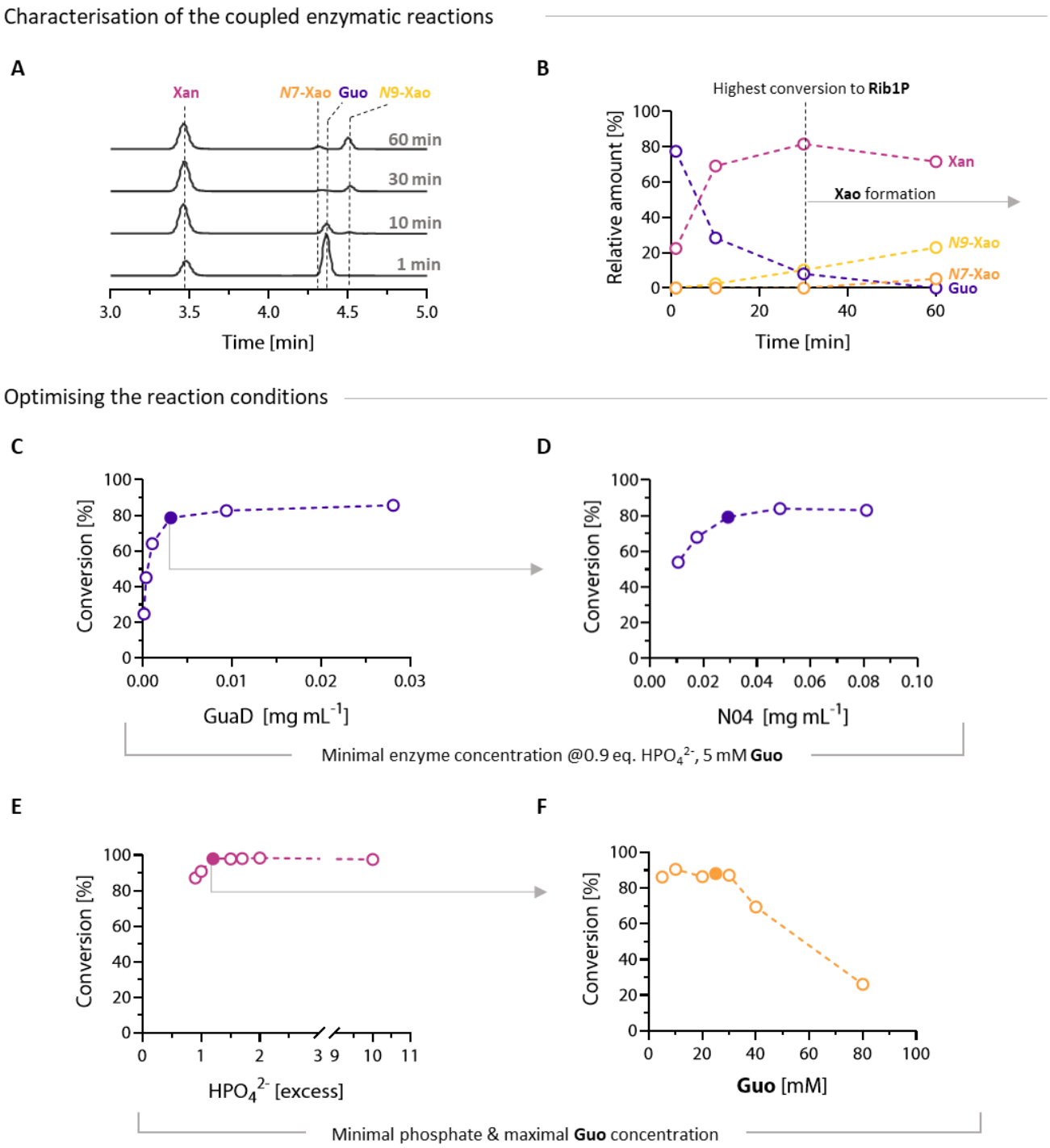

Figure 2. GuaD coupled synthesis of **Rib1P**. A) Representative HPLC chromatograms (recorded at λ = 260 nm) show the time course of the PNP N04 and *Dg*DuaD biocatalytic cascade. Please note the different extinction coefficients of the nucleosides and nucleobases (*Figure S11*). B) Time course of the conversion of **Guo** to **Xan** and the byproducts ***N*9-Xao** and ***N*7-Xao.** C-F) Optimization of the PNP/GuaD cascade by varying *Dg*GuaD concentrations (C), N04 concentrations (D), phosphate concentrations (E) and **Guo** concentration (F). Full-marked points represent the best conditions used for further experiments.

Despite *Dg*GuaD's high selectivity, this cascade proved to be under kinetic control due to a low degree of promiscuity of PNPs. As such, we observed additional byproducts in addition to **Xan** arising from the glycosylation of **Xan** to give either ***N*9-Xao** or, as recently discovered, ***N*7-Xao**.[44] Although N04 proved to be the most **Guo**-selective enzyme among those we screened, minor amounts of byproduct formation (**Xan** glycosides) were unavoidable (*Figure S10-11*). Therefore, we decided to stop the reactions at the maximum **Xan** concentration (the highest conversion point to **Rib1P**). This is crucial as the final reaction equilibrium forms between **Xan** and **Xao**, thereby minimising available **Rib1P** levels (*Figure 2B*).

Based on these preliminary results, we optimised the reaction conditions to generate maximum **Rib1P** concentrations. We determined the optimum ratio of the two enzymes under cascade reactions. This involved directly reducing the *Dg*GuaD concentration while maintaining a fixed N04 concentration (with 5 mM **Guo** and 0.9 eq. HPO_4^{2-}). The process was then repeated with the optimum *Dg*GuaD concentration but with varying N04 catalyst loads (*Figure 2C-D*). To further improve **Guo** cleavage, we studied the impact of increasing phosphate eq. on the enzymatic cascade. To achieve near-full **Guo** cleavage of >98%, only 1.2 eq. of phosphate was required (*Figure 2E*). For comparison, the phosphorolysis of **Guo** would require 1150 eq. of phosphate for 98% conversion (with a K = 0.04 of **Guo** at 50 °C). Since phosphate removal is one of the most critical steps in the production of **Rib1P**,[24] this is a significant improvement over the available enzymatic production methods based on natural substrates. Finally, we determined the maximum **Guo** loading in the reactions. Reactions with **Guo** concentrations >40 mM never completely dissolved (data not shown), and maximum **Guo** conversion significantly decreased (*Figure 2F*). Therefore, 25 mM **Guo** was applied for further experiments as all reactants fully dissolved within 15 min (data not shown). Intriguingly, the apparent solubility of **Guo** and **Xan** up to 30 mM was drastically higher than that in enzyme-free systems (the experimentally determined solubilities were 3.6 mM for **Guo** and 0.2 mM for **Xan** at 50 °C in H_2O). These differences might be explained by the higher pH applied in enzymatic reactions (**Xan** solubility is highly pH-dependent[45]) or the formation of soluble oligomers, as discussed for **Gua**.[46]

Production of ribose-1-P at the gram scale

Following optimisation, we aimed to produce **Rib1P** as a barium salt at the gram scale. Therefore, we performed a test run on a 2 mL scale (*Figure S12*) to determine when to terminate the reaction and then upscaled the reaction volume to 150 mL. After the up-scaled reaction was stopped at a conversion of 88%, the enzyme was removed by freezing and thawing the reaction mixture (*Figure 4A*). Taking advantage of the pH-dependent solubility, free **Xan** was precipitated by shifting the pH to ≈7 (*Figure 4A-B*). At this step, approximately 2% of the initial **Xan** remained in the mixture, but ***N*9-Xao** was only slightly affected by the pH shift (as determined by HPLC). Further purification was based on our previously published method.[24] Phosphate was precipitated using NH_4Cl and $MgCl_2$. Due to the low phosphate concentration, the need for phosphate-precipitating compounds has been significantly minimised, which reduced the co-precipitation (and therefore loss) of **Rib1P**. Finally, after confirming phosphate precipitation (*Figure S13*), **Rib1P** was precipitated as its Ba-salt by the addition of ethanol and barium acetate. For the collection of the precipitated **Rib1P**, we compared filtration and centrifugation. Although centrifugation was more prone to residual ethanol contamination, it yielded more **Rib1P** and was the preferred method due to handling benefits (*Figure S14, Table S2*). Using centrifugation**, Rib1P** was obtained with an isolated yield of up to 79% (1.1 g) and a purity of 94% (as determined by quantitative ^{1}H-NMR, see SI for NMR data). The main impurities were acetate, ethanol and ***N*9-Xao** (*Table S2*). Although the pH shift did not strongly impact the ***N*9-Xao** concentration, its precipitation occurred progressively during the purification process due to incubation steps at low temperatures (*Figure 4B*), resulting in values less than 1% in the final **Rib1P** stock (*Table S2*).

To validate the compatibility of the **Rib1P** obtained via this cascade, we used the produced material in three enzymatic glycosylation reactions with different halogenated uridine bases (**5-F-**

Ura, **5-Br-Ura**, **5-I-Ura**). Conversions were between 65 and 75% with an equimolar concentration of **Rib1P** compared to the halogenated nucleobases and matched well with calculated conversions based on the available equilibrium constants (*Figure 4C*).[16] This demonstrates that our **Rib1P** can be used to synthesise modified nucleoside analogues and can be envisioned as being applied to difficult-to-access products, as recently shown for 5-ethynyluridine.[17]

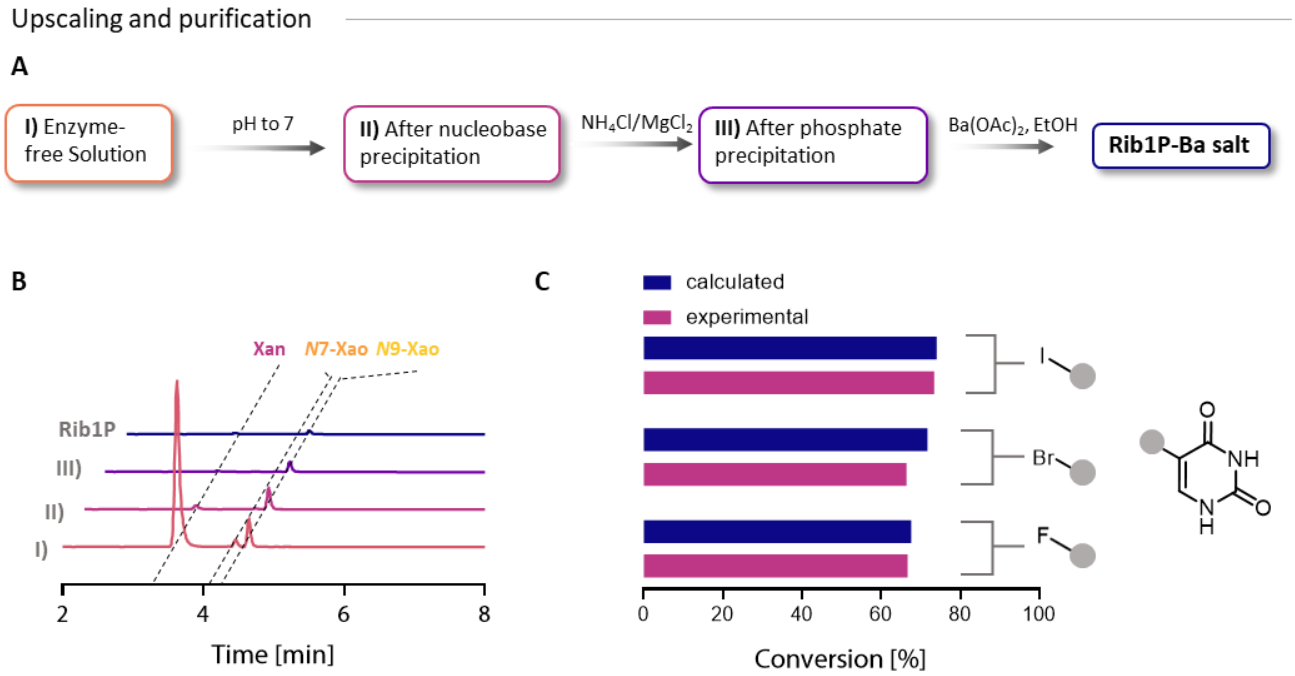

Figure 3. Purification and gram-scale synthesis of **Rib1P**. A) Purification process B) Corresponding HPLC chromatograms for the purification steps (recorded at λ = 260 nm). Please note the different extinction coefficients of the nucleosides and -bases (*Figure S11*). C) Experimental validation of **Rib1P** identity via direct glycosylation of halogenated pyrimidines. The calculated values were taken from the ref[16].

Environmental impact of ribose-1-P synthesis routes

To estimate the environmental burden of (chemo)enzymatic **Rib1P** synthesis routes, we compared our cascade approach with other published methods that are i) NP-based, ii) use available substrates and enzymes, and iii) give straightforward access to crystalline **Rib1P**-salts. Hence, the methods described by Kamel *et al.*[24] and Fateev *et al.*[23] (enzymatic approach starting from uridine) and by Varizhuk *et al.*[29] (chemoenzymatic method starting from **7-Me-Guo**) were selected. Both the CHEM21 Zero Pass tool[47] and E-factor calculations[48–50] were applied. CHEM21 Zero Pass allows for a simple evaluation of reactions with a flag system and can thereby evaluate reactions in early development. To different categories, the following flags are assigned: i) green flag (good to go, >89%), ii) amber flag (acceptable, some issues, 70-89%), and iii) red flag (indicate the discontinuation of the method, <70%). To make the table more accessible for people with colour deficiencies,[51] the colours were changed from green, yellow, and red to yellow, orange, and red, respectively. However, as the stoichiometry, yield, and solvent do not impact the atom economy (AE) included in the CHEM21 Zero Pass tool, we were further interested in comparing the different methods by the E-factor. Here, the amount of waste is calculated per weight unit of product produced (simple E-factor, sEF), which can be expanded by considering solvents and water consumption (complete E-factor, cEF).

When analysing the three published methods with the CHEM21 tool, they created a red flag because of either low yields (Kamel *et al.* and Fateev *et al.*) or the need for toxic chemicals (Varizhuk *et al*.) (*Table 1*). Indeed, dichloromethane, dimethylformamide, and diethyl ether are listed as highly avoidable solvents,[52] and iodomethane causes severe environmental concerns (H410). In contrast, the biocatalytic cascade reported herein did not generate red flags for any categories.

E-factor calculations for all four methods (detailed information is provided in the SI) demonstrated that our cascade approach showed the lowest sEF (0.9 vs 3.7, 8.9 and 5.1). In contrast, the cEF of our method was by factors of ~3.0 and ~1.5 higher compared to the methods described by Kamel *et al.* and Fateev *et al.* (*Table 1*). However, a ~3.3-fold reduction in the cEF was obtained compared to the other high-yielding chemoenzymatic approach described by Varizhuk *et al.*. Solvents for purification and isolation of **Rib1P** had by far the most significant impact on the cEF values, as is typical for workup procedures.[53] Therefore, future studies should focus on reducing the use of solvents (including water), e.g., by optimising the downstream processing or achieving even higher substrate loadings (e.g., by running slurry-to-slurry reactions).

Table 1. Evaluation of the biocatalytic cascade for synthesising ribose-1-phosphate.

	Chem21 tool						Waste production	
	Yield [%]	Conv. [%]	S [%]	AE [%]	Solvents	Health & Safety	sEF	cEF
Fateev *et al.*[23]	31	34	92	77	no flag	no flag	5.1	570
Kamel *et al.*[24]	25	40	63	77	no flag	no flag	8.9	285
Varizhuk *et al.*[29]	79	99	80	56	Et_2O, DMF, DCM	DMF,MeI	3.7	2816
This work	79	88	90	71	no flag	no flag	0.9	847

Conv. = conversion, S = selectivity, AE = atom economy, EtOH = ethanol, DMF = *N*,*N*-dimethylformamide, DCM = dichloromethane, Et_2O = diethyl ether, MeI = iodomethane. sEF = simple E-factor, cEF = complete E-factor. The colours of the Chem21 tool were changed for accessibility.

Conclusion

In conclusion, we present an improved biocatalytic process for the one-pot synthesis of **Rib1P**. By coupling a selective guanine deaminase to the NP-catalysed **Guo** cleavage, **Gua** was efficiently deaminated to **Xan**, hence shifting the reaction towards almost complete **Guo** cleavage. We demonstrate that this biocatalytic approach decreases the need for toxic reagents and purification steps, reducing the overall environmental burden of **Rib1P** synthesis. Due to the wide substrate spectrum of NPs, our approach offers the opportunity to produce a wide range of P1Ps. We expect our work to facilitate biocatalytic access to many sought-after nucleoside analogues by providing straightforward access to P1Ps as springboard synthons.

Author contributions (with the CRediT definitions as recommended by Brand *et al.*[54])

Conceptualisation: JM, SW, FK, and AK; Data curation: JM; Formal analysis: JM, LN, and AD; Funding acquisition: PN and AK; Investigation: JM, JB, CB, AD, LN, and SK; Methodology: JM, SW, AK; Project administration: PN and AK; Resources: PN and AK; Software: −; Supervision: SW, FK, PN and AK; Validation: −; Visualisation: JM; Writing-original draft: JM; Writing-Review & Editing: all authors.

Data availability statement

The supplementary material and experiments are in the Supplementary Information. Additionally, all raw MS and NMR data, as well as each figure's source data (when applicable) from the main manuscript and SI, are freely available externally at zenodo.org (10.5281/zenodo.10604601)[55].

Acknowledgements

The authors thank Samantha Voges (TU Berlin, NMR Department) for assistance with NMR analyses. We additionally thank the Center for Mass Spectrometry at TU Berlin for HRMS analyses. Further, we thank Sarah Kamel for providing information on her synthesis protocols.

Accessibility Statement

The data presented in this manuscript are depicted using scientific colour maps. Since ca. 4% of the human population is colour vision-deficient, we made a conscious effort to avoid unscientific uses of colour, such as colour ambiguities and other biases that could lead to misrepresentation, limited accessibility, or loss of information upon reduction of the colour space.[51] Thus, all figures herein were created using the scientific colour map *plasma* or *viridis*, which retains colour-coded information for all readers.

Conflict of interest

AK is the CEO of the biotech company BioNukleo GmbH. SW was a scientist at BioNukleo GmbH, and PN is an advisory board member. At the time of the conceptualisation of this work, FK was a scientist at BioNukleo GmbH. The remaining authors declare no conflicts of interest.

Author information

Corresponding Author
Dr. Anke Kurreck,
orcid.org/0000-0001-6919-725X
anke.wagner@tu-berlin.de

Other Authors
Jonas Motter, orcid.org/0000-0002-7154-9119
Sarah Westarp, orcid.org/0000-0001-6498-8810
Jonas Barsig, orcid.org/0009-0009-6787-6967
Christina Betz, orcid.org/0009-0004-8404-2183
Amin Dagane
Dr. Felix Kaspar, orcid.org/0000-0001-6391-043X
Lena Neumair orcid.org/0009-0008-5904-0791
Dr. Sebastian Kemper, orcid.org/0000-0003-0192-518X
Dr. Peter Neubauer, orcid.org/0000-0002-1214-9713

References

(1) Alexeev, C. S.; Drenichev, M. S.; Dorinova, E. O.; Esipov, R. S.; Kulikova, I. V.; Mikhailov, S. N. Use of Nucleoside Phosphorylases for the Preparation of 5-Modified Pyrimidine Ribonucleosides. *Biochimica et Biophysica Acta (BBA) - Proteins and Proteomics* **2020**, *1868* (1), 140292. https://doi.org/10.1016/j.bbapap.2019.140292.

(2) Liu, G.; Cheng, T.; Chu, J.; Li, S.; He, B. Efficient Synthesis of Purine Nucleoside Analogs by a New Trimeric Purine Nucleoside Phosphorylase from Aneurinibacillus Migulanus AM007. *Molecules* **2020**, *25* (1), 100. https://doi.org/10.3390/molecules25010100.

(3) Yehia, H.; Kamel, S.; Paulick, K.; Neubauer, P.; Wagner, A. Substrate Spectra of Nucleoside Phosphorylases and Their Potential in the Production of Pharmaceutically Active Compounds. *Current Pharmaceutical Design* **2017**, *23* (45), 6913–6935. https://doi.org/10.2174/1381612823666171024155811.

(4) Yehia, H.; Westarp, S.; Röhrs, V.; Kaspar, F.; Giessmann, R. T.; Klare, H. F. T.; Paulick, K.; Neubauer, P.; Kurreck, J.; Wagner, A. Efficient Biocatalytic Synthesis of Dihalogenated Purine Nucleoside Analogues Applying Thermodynamic Calculations. *Molecules* **2020**, *25* (4), 934. https://doi.org/10.3390/molecules25040934.

(5) Denisova, A. O.; Tokunova, Y. A.; Fateev, I. V.; Breslav, A. A.; Leonov, V. N.; Dorofeeva, E. V.; Lutonina, O. I.; Muzyka, I. S.; Esipov, R. S.; Kayushin, A. L.; Konstantinova, I. D.; Miroshnikov, A. I.; Stepchenko, V. A.; Mikhailopulo, I. A. The Chemoenzymatic Synthesis of 2-Chloro- and 2-Fluorocordycepins. *Synthesis-Stuttgart* **2017**, *49* (21), 4853–4860. https://doi.org/10.1055/s-0036-1590804.

(6) Krenitsky, T. A.; Koszalka, G. W.; Tuttle, J. V. Purine Nucleoside Synthesis: An Efficient Method Employing Nucleoside Phosphorylases. *Biochemistry* **1981**, *20* (12), 3615–3621. https://doi.org/10.1021/bi00515a048.

(7) Westarp, S.; Benckendorff, C.; Motter, J.; Rohrs, V.; Sanghvi, Y.; Neubauer, P.; Kurreck, J.; Kurreck, A.; Miller, G. J. Biocatalytic Nucleobase Diversification of 4'-Thionucleosides and Application of Derived 5-Ethynyl-4'-Thiouridine for RNA Synthesis Detection. *Angewandte Chemie International Edition n/a* (n/a), e202405040. https://doi.org/10.1002/anie.202405040.

(8) Kataev, V. E.; Garifullin, B. F. Antiviral Nucleoside Analogs. *Chem Heterocycl Comp* **2021**, *57* (4), 326–341. https://doi.org/10.1007/s10593-021-02912-8.

(9) Seley-Radtke, K. L.; Yates, M. K. The Evolution of Nucleoside Analogue Antivirals: A Review for Chemists and Non-Chemists. Part 1: Early Structural Modifications to the Nucleoside Scaffold. *Antiviral Research* **2018**, *154*, 66–86. https://doi.org/10.1016/j.antiviral.2018.04.004.

(10) Guinan, M.; Benckendorff, C.; Smith, M.; Miller, G. J. Recent Advances in the Chemical Synthesis and Evaluation of Anticancer Nucleoside Analogues. *Molecules* **2020**, *25* (9), 2050. https://doi.org/10.3390/molecules25092050.

(11) Galmarini, C. M.; Mackey, J. R.; Dumontet, C. Nucleoside Analogues and Nucleobases in Cancer Treatment. *The Lancet Oncology* **2002**, *3* (7), 415–424. https://doi.org/10.1016/S1470-2045(02)00788-X.

(12) Morais, P.; Adachi, H.; Yu, Y.-T. The Critical Contribution of Pseudouridine to mRNA COVID-19 Vaccines. *Frontiers in Cell and Developmental Biology* **2021**, *9*.

(13) Pardi, N.; Hogan, M. J.; Porter, F. W.; Weissman, D. mRNA Vaccines — a New Era in Vaccinology. *Nat Rev Drug Discov* **2018**, *17* (4), 261–279. https://doi.org/10.1038/nrd.2017.243.

(14) Motter, J.; Benckendorff, C. M. M.; Westarp, S.; Sunde-Brown, P.; Neubauer, P.; Kurreck, A.; Miller, G. J. Purine Nucleoside Antibiotics: Recent Synthetic Advances Harnessing Chemistry and Biology. *Nat. Prod. Rep.* **2024**. https://doi.org/10.1039/D3NP00051F.

(15) Thomson, J. M.; Lamont, I. L. Nucleoside Analogues as Antibacterial Agents. *Frontiers in Microbiology* **2019**, *10*. https://doi.org/10.3389/fmicb.2019.00952.

(16) Kaspar, F.; Giessmann, R. T.; Neubauer, P.; Wagner, A.; Gimpel, M. Thermodynamic Reaction Control of Nucleoside Phosphorolysis. *Advanced Synthesis & Catalysis* **2020**, *362* (4), 867–876. https://doi.org/10.1002/adsc.201901230.

(17) Kaspar, F.; Brandt, F.; Westarp, S.; Eilert, L.; Kemper, S.; Kurreck, A.; Neubauer, P.; Jacob, C. R.; Schallmey, A. Biased Borate Esterification during Nucleoside Phosphorylase-Catalyzed

Reactions: Apparent Equilibrium Shifts and Kinetic Implications**. *Angewandte Chemie International Edition* **2023**, *62* (20), e202218492. https://doi.org/10.1002/anie.202218492.
(18) Kaspar, F.; Giessmann, R. T.; Hellendahl, K. F.; Neubauer, P.; Wagner, A.; Gimpel, M. General Principles for Yield Optimization of Nucleoside Phosphorylase-Catalyzed Transglycosylations. *ChemBioChem* **2020**, *21* (10), 1428–1432. https://doi.org/10.1002/cbic.201900740.
(19) Hellendahl, K. F.; Kaspar, F.; Zhou, X.; Yang, Z.; Huang, Z.; Neubauer, P.; Kurreck, A. Optimized Biocatalytic Synthesis of 2-Selenopyrimidine Nucleosides by Transglycosylation**. *ChemBioChem* **2021**, *22* (11), 2002–2009. https://doi.org/10.1002/cbic.202100067.
(20) McIntosh, J. A.; Benkovics, T.; Silverman, S. M.; Huffman, M. A.; Kong, J.; Maligres, P. E.; Itoh, T.; Yang, H.; Verma, D.; Pan, W.; Ho, H.-I.; Vroom, J.; Knight, A. M.; Hurtak, J. A.; Klapars, A.; Fryszkowska, A.; Morris, W. J.; Strotman, N. A.; Murphy, G. S.; Maloney, K. M.; Fier, P. S. Engineered Ribosyl-1-Kinase Enables Concise Synthesis of Molnupiravir, an Antiviral for COVID-19. *ACS Cent. Sci.* **2021**, *7* (12), 1980–1985. https://doi.org/10.1021/acscentsci.1c00608.
(21) Huffman, M. A.; Fryszkowska, A.; Alvizo, O.; Borra-Garske, M.; Campos, K. R.; Canada, K. A.; Devine, P. N.; Duan, D.; Forstater, J. H.; Grosser, S. T.; Halsey, H. M.; Hughes, G. J.; Jo, J.; Joyce, L. A.; Kolev, J. N.; Liang, J.; Maloney, K. M.; Mann, B. F.; Marshall, N. M.; McLaughlin, M.; Moore, J. C.; Murphy, G. S.; Nawrat, C. C.; Nazor, J.; Novick, S.; Patel, N. R.; Rodriguez-Granillo, A.; Robaire, S. A.; Sherer, E. C.; Truppo, M. D.; Whittaker, A. M.; Verma, D.; Xiao, L.; Xu, Y.; Yang, H. Design of an in Vitro Biocatalytic Cascade for the Manufacture of Islatravir. *Science* **2019**, *366* (6470), 1255–1259. https://doi.org/10.1126/science.aay8484.
(22) Tener, G.; Wright, R.; Khorana, H. A Synthesis of Alpha-D-Ribofuranose-1-Phosphate. *J. Am. Chem. Soc.* **1956**, *78* (2), 506–507. https://doi.org/10.1021/ja01583a078.
(23) Fateev, I. V.; Kharitonova, M. I.; Antonov, K. V.; Konstantinova, I. D.; Stepanenko, V. N.; Esipov, R. S.; Seela, F.; Temburnikar, K. W.; Seley-Radtke, K. L.; Stepchenko, V. A.; Sokolov, Y. A.; Miroshnikov, A. I.; Mikhailopulo, I. A. Recognition of Artificial Nucleobases by E. Coli Purine Nucleoside Phosphorylase versus Its Ser90Ala Mutant in the Synthesis of Base-Modified Nucleosides. *Chemistry – A European Journal* **2015**, *21* (38), 13401–13419. https://doi.org/10.1002/chem.201501334.
(24) Kamel, S.; Weiß, M.; Klare, H. F. T.; Mikhailopulo, I. A.; Neubauer, P.; Wagner, A. Chemo-Enzymatic Synthesis of α-d-Pentofuranose-1-Phosphates Using Thermostable Pyrimidine Nucleoside Phosphorylases. *Molecular Catalysis* **2018**, *458*, 52–59. https://doi.org/10.1016/j.mcat.2018.07.028.
(25) Kalckar, H. M. The Enzymatic Synthesis of Purine Ribosides. *Journal of Biological Chemistry* **1947**, *167* (2), 477–486. https://doi.org/10.1016/S0021-9258(17)31000-1.
(26) Artsemyeva, J. N.; Remeeva, E. A.; Buravskaya, T. N.; Konstantinova, I. D.; Esipov, R. S.; Miroshnikov, A. I.; Litvinko, N. M.; Mikhailopulo, I. A. Anion Exchange Resins in Phosphate Form as Versatile Carriers for the Reactions Catalyzed by Nucleoside Phosphorylases. *Beilstein J. Org. Chem.* **2020**, *16* (1), 2607–2622. https://doi.org/10.3762/bjoc.16.212.
(27) Zhang, W.; Turney, T.; Surjancev, I.; Serianni, A. S. Enzymatic Synthesis of Ribo- and 2′-Deoxyribonucleosides from Glycofuranosyl Phosphates: An Approach to Facilitate Isotopic Labeling. *Carbohydrate Research* **2017**, *449*, 125–133. https://doi.org/10.1016/j.carres.2017.07.006.
(28) Kulikova, I. V.; Drenichev, M. S.; Solyev, P. N.; Alexeev, C. S.; Mikhailov, S. N. Enzymatic Synthesis of 2-Deoxyribose 1-Phosphate and Ribose 1 Phosphate and Subsequent Preparation of Nucleosides. *European Journal of Organic Chemistry* **2019**, *2019* (41), 6999–7004. https://doi.org/10.1002/ejoc.201901454.
(29) Varizhuk, I. V.; Oslovsky, V. E.; Solyev, P. N.; Drenichev, M. S.; Mikhailov, S. N. Synthesis of α-D-Ribose 1-Phosphate and 2-Deoxy-α-D-Ribose 1-Phosphate Via Enzymatic Phosphorolysis of 7-Methylguanosine and 7-Methyldeoxyguanosine. *Current Protocols* **2022**, *2* (1), e347. https://doi.org/10.1002/cpz1.347.
(30) Beyaztaş, S.; Arslan, O. Purification of Xanthine Oxidase from Bovine Milk by Affinity Chromatography with a Novel Gel. *Journal of Enzyme Inhibition and Medicinal Chemistry* **2015**, *30* (3), 442–447. https://doi.org/10.3109/14756366.2014.943204.

(31) Chen, C.; Cheng, G.; Hao, H.; Dai, M.; Wang, X.; Huang, L.; Liu, Z.; Yuan, Z. Mechanism of Porcine Liver Xanthine Oxidoreductase Mediated N-Oxide Reduction of Cyadox as Revealed by Docking and Mutagenesis Studies. *PLOS ONE* **2013**, *8* (9), e73912. https://doi.org/10.1371/journal.pone.0073912.
(32) Rashidi, M. R.; Soruraddin, M. H.; Taherzadeh, F.; Jouyban, A. Catalytic Activity and Stability of Xanthine Oxidase in Aqueous-Organic Mixtures. *Biochemistry Moscow* **2009**, *74* (1), 97–101. https://doi.org/10.1134/S0006297909010155.
(33) Wang, C.-H.; Zhao, T.-X.; Li, M.; Zhang, C.; Xing, X.-H. Characterization of a Novel Acinetobacter Baumannii Xanthine Dehydrogenase Expressed in Escherichia Coli. *Biotechnol Lett* **2016**, *38* (2), 337–344. https://doi.org/10.1007/s10529-015-1986-y.
(34) Zarepour, M.; Kaspari, K.; Stagge, S.; Rethmeier, R.; Mendel, R. R.; Bittner, F. Xanthine Dehydrogenase AtXDH1 from Arabidopsis Thaliana Is a Potent Producer of Superoxide Anions via Its NADH Oxidase Activity. *Plant Mol Biol* **2010**, *72* (3), 301–310. https://doi.org/10.1007/s11103-009-9570-2.
(35) Leimkühler, S.; Hodson, R.; George, G. N.; Rajagopalan, K. V. Recombinant Rhodobacter Capsulatus Xanthine Dehydrogenase, a Useful Model System for the Characterization of Protein Variants Leading to Xanthinuria I in Humans *. *Journal of Biological Chemistry* **2003**, *278* (23), 20802–20811. https://doi.org/10.1074/jbc.M303091200.
(36) Kunka, A.; Marques, S. M.; Havlasek, M.; Vasina, M.; Velatova, N.; Cengelova, L.; Kovar, D.; Damborsky, J.; Marek, M.; Bednar, D.; Prokop, Z. Advancing Enzyme's Stability and Catalytic Efficiency through Synergy of Force-Field Calculations, Evolutionary Analysis, and Machine Learning. *ACS Catal.* **2023**, *13* (19), 12506–12518. https://doi.org/10.1021/acscatal.3c02575.
(37) Peccati, F.; Alunno-Rufini, S.; Jiménez-Osés, G. Accurate Prediction of Enzyme Thermostabilization with Rosetta Using AlphaFold Ensembles. *J. Chem. Inf. Model.* **2023**, *63* (3), 898–909. https://doi.org/10.1021/acs.jcim.2c01083.
(38) Wu, H.; Chen, Q.; Zhang, W.; Mu, W. Overview of Strategies for Developing High Thermostability Industrial Enzymes: Discovery, Mechanism, Modification and Challenges. *Critical Reviews in Food Science and Nutrition* **2023**, *63* (14), 2057–2073. https://doi.org/10.1080/10408398.2021.1970508.
(39) Vieille, C.; Zeikus, G. J. Hyperthermophilic Enzymes: Sources, Uses, and Molecular Mechanisms for Thermostability. *Microbiology and Molecular Biology Reviews* **2001**, *65* (1), 1–43. https://doi.org/10.1128/mmbr.65.1.1-43.2001.
(40) Zamost, B. L.; Nielsen, H. K.; Starnes, R. L. Thermostable Enzymes for Industrial Applications. *Journal of Industrial Microbiology* **1991**, *8* (2), 71–81. https://doi.org/10.1007/BF01578757.
(41) Gupta, N. K.; Glantz, M. D. Isolation and Characterization of Human Liver Guanine Deaminase. *Archives of Biochemistry and Biophysics* **1985**, *236* (1), 266–276. https://doi.org/10.1016/0003-9861(85)90626-5.
(42) Mahor, D.; Prasad, G. S. Biochemical Characterization of Kluyveromyces Lactis Adenine Deaminase and Guanine Deaminase and Their Potential Application in Lowering Purine Content in Beer. *Frontiers in Bioengineering and Biotechnology* **2018**, *6*.
(43) Kim, J.; Park, S. I.; Ahn, C.; Kim, H.; Yim, J. Guanine Deaminase Functions as Dihydropterin Deaminase in the Biosynthesis of Aurodrosopterin, a Minor Red Eye Pigment of Drosophila. *J Biol Chem* **2009**, *284* (35), 23426–23435. https://doi.org/10.1074/jbc.M109.016493.
(44) Westarp, S.; Brandt, F.; Neumair, L.; Betz, C.; Dagane, A.; Kemper, S.; Jacob, C. R.; Neubauer, P.; Kurreck, A.; Kaspar, F. Nucleoside Phosphorylases Make N7-Xanthosine. *Nat Commun* **2024**, *15* (1), 3625. https://doi.org/10.1038/s41467-024-47287-4.
(45) Lister, J. H.; Caldbick, D. S. An Investigation into the Factors Governing the Aqueous Solubility of Xanthine (Purine-2,6-Dione). *Journal of Applied Chemistry and Biotechnology* **1976**, *26* (1), 351–354. https://doi.org/10.1002/jctb.5020260151.
(46) Hirano, A.; Tokunaga, H.; Tokunaga, M.; Arakawa, T.; Shiraki, K. The Solubility of Nucleobases in Aqueous Arginine Solutions. *Archives of Biochemistry and Biophysics* **2010**, *497* (1), 90–96. https://doi.org/10.1016/j.abb.2010.03.009.
(47) McElroy, C. R.; Constantinou, A.; Jones, L. C.; Summerton, L.; Clark, J. H. Towards a Holistic Approach to Metrics for the 21st Century Pharmaceutical Industry. *Green Chem.* **2015**, *17* (5), 3111–3121. https://doi.org/10.1039/C5GC00340G.

(48) Kaspar, F.; Stone, M. R. L.; Neubauer, P.; Kurreck, A. Route Efficiency Assessment and Review of the Synthesis of β-Nucleosides via N-Glycosylation of Nucleobases. *Green Chem.* **2021**, *23* (1), 37–50. https://doi.org/10.1039/D0GC02665D.
(49) A. Sheldon, R. The E Factor: Fifteen Years On. *Green Chemistry* **2007**, *9* (12), 1273–1283. https://doi.org/10.1039/B713736M.
(50) A. Sheldon, R. The E Factor 25 Years on: The Rise of Green Chemistry and Sustainability. *Green Chemistry* **2017**, *19* (1), 18–43. https://doi.org/10.1039/C6GC02157C.
(51) Kaspar, F.; Crameri, F. Coloring Chemistry—How Mindful Color Choices Improve Chemical Communication. *Angewandte Chemie International Edition* **2022**, *61* (16), e202114910. https://doi.org/10.1002/anie.202114910.
(52) Prat, D.; Wells, A.; Hayler, J.; Sneddon, H.; McElroy, C. R.; Abou-Shehada, S.; Dunn, P. J. CHEM21 Selection Guide of Classical- and Less Classical-Solvents. *Green Chem.* **2015**, *18* (1), 288–296. https://doi.org/10.1039/C5GC01008J.
(53) Kaspar, F.; Stone, M. R. L.; Neubauer, P.; Kurreck, A. Route Efficiency Assessment and Review of the Synthesis of β-Nucleosides via N-Glycosylation of Nucleobases. *Green Chem.* **2021**, *23* (1), 37–50. https://doi.org/10.1039/D0GC02665D.
(54) Brand, A.; Allen, L.; Altman, M.; Hlava, M.; Scott, J. Beyond Authorship: Attribution, Contribution, Collaboration, and Credit. *Learned Publishing* **2015**, *28*. https://doi.org/10.1087/20150211.
(55) Motter, J. Data for “A Deamination-Driven Biocatalytic Cascade for the Synthesis of Ribose-1-Phosphate,” 2024. https://doi.org/10.5281/zenodo.10604602.